A
REPORT ON

CFD SIMULATION OF MIXING AND SEGREGATION IN A TAPERED FLUIDIZED BED

A REPORT SUBMITTED IN PARTIAL FULFILLMENT OF THE REQUIREMENTS FOR THE DEGREE OF

BACHELOR OF TECHNOLOGY (CHEMICAL ENGINEERING)

Submitted By
DEEPALI PATRO
Roll No. : 10400019

Department of Chemical Engineering
National Institute of Technology
Rourkela

A

REPORT ON

CFD SIMULATION OF MIXING AND SEGREGATION IN A TAPERED FLUIDIZED BED

A REPORT SUBMITTED IN PARTIAL FULFILLMENT OF THE REQUIREMENTS FOR THE DEGREE OF

BACHELOR OF TECHNOLOGY (CHEMICAL ENGINEERING)

Submitted By

DEEPALI PATRO

Roll No. : 10400019

Under the guidance of

Prof. (Dr.) K. C. Biswal

Department of Chemical Engineering

National Institute of Technology

Rourkela

National Institute of Technology

Rourkela

CERTIFICATE

This is to certify that that the work in this thesis report entitled "**CFD Simulation Of Mixing And Segregation In A Tapered Fluidized Bed**" submitted by **Deepali Patro** in partial fulfillment of the requirements for the degree of Bachelor of Technology in Chemical Engineering, Session 2004-2008 in the department of Chemical Engineering, National Institute of Technology, Rourkela, is an authentic work carried out by her under my supervision and guidance.

To the best of my knowledge the matter embodied in the report has not been submitted to any other University /Institute for the award of any degree.

Date:

Dr. K. C. Biswal
Department of Chemical Engineering
National Institute of Technology
Rourkela – 769008

ACKNOWLEDGEMENT

I wish to express my sincere thanks and gratitude to **Prof (Dr.) K. C. Biswal** for suggesting me the topic and providing me the guidance, motivation and constructive criticism throughout the course of the project.

I thank Prof. (**Dr.) R. K. Singh** for acting as the project coordinator.

I am grateful to Prof. (Dr.) K. C. Biswal, Head of the Department, Chemical Engineering for providing me the necessary opportunities for the completion of my project. I also thank other staff members of my department for their invaluable help and guidance.

Deepali Patro

Date: Roll No. 10400019

B.Tech.

Chemical Engineering

CONTENTS

LIST OF FIGURES

LIST OF TABLES

ABSTRACT

Fluidization of different materials results either in a well-mixed or a segregated bed. Depending upon the operating conditions, smaller particles (floatsam) tend to rise to the bed, and larger particles (jetsam) tend to sink to the bottom of the bed. The tapered fluidized bed can be used to overcome certain draw backs of the gas-solid system because of the fact that a velocity gradient exists along the axial direction of the bed with increase in cross-sectional area. To study the dynamic characteristics of the homogenous mixture of regular and irregular particles several experiments have been carried out with varying compositions.The particle flow pattern and granule segregation in tapered fluidized bed have been studied by first fluidizing the beds of varying total mass and granule fractions and then defluidize them suddenly to freeze the composition, section the bed in layers, and determine the composition in each layer by sieving. A series of unsteady, three-fluid CFD simulations were performed using FLUENT^{TM} 6.2. Simulation parameters viz. solution technique, grid, maximum packing fraction and operating conditions like gas velocity were each investigated for the relative effects on particle mixing and segregation. Good agreement of solid volume fraction profile was obtained between the experimental results and simulation results for regular particles (glass beads).

CHAPTER 1

INTRODUCTION

1. INTRODUCTION:

Fluidization is the operation by which solid particles are transformed into a fluid-like state through suspension in a gas or liquid. One of the most prominent features of fluidized beds is their ability to mix and segregate. This is of great importance for many industrial processes. Knowledge of particulate mixing and segregation would be very useful in the design of fluidized bed reactors as well as in predicting mass transfer, heat transfer and reaction rates, erosion, and concentration profiles. Mixing of fluid and particles promotes gas-particle surface contact and uniformity of temperature of chemical reactants.

Most of the gas-solid fluidization behavior studies that have been reported are for straight cylindrical or columnar fluidized beds, although a considerable proportion of the fluidized beds have inclined walls or have a tapered bottom section. A velocity gradient exists in the axial direction in tapered bed leading to unique dynamic characteristics of the bed. Due to this characteristic, tapered fluidized beds have found wide applicability in many industrial processes such as, waste water treatment (Shi et al.,1984) immobilized biofilm reaction, incineration of waste materials, coating of nuclear fuel particles, crystallization, coal gasification, roasting sulfide ores (Peng and Fan,1997) and food processing (Depypere et al.,2005) etc. Tapered fluidized beds are very useful for fluidization of materials with a wide particle size distribution, as well as for exothermic reactions (Kim et al., 2000). They can be operated smoothly without any instability i.e. with less pressure fluctuations (Shi et al., 1984) and also for extensive particle mixing (Schaafsma et al. 2006). Despite their widespread application, much of the development and design of tapered fluidized bed reactors have been empirical as the complex behavior of gas–solid flow in these systems makes flow modeling a challenging task. In addition, numerical solutions of complex non-linear equations, with moving phase boundaries, are difficult to obtain.

CFD is used for predicting the quantitative results, when fluid flows, in operations involving Simultaneous flow of heat, Mass transfer, Phase change (e.g. melting, freezing), Chemical reactions(e.g. combustion), Mechanical movement(e.g. piston ,fans), Stress & displacement etc. Of the various modeling tools, computational fluid dynamics (CFD) is the most promising for future fluidized bed modelling. CFD is intended to include the key mechanisms of importance to predict accurate flow and other characteristics of fluidized beds for design, scale-up and optimization. With increasing computational capabilities and computational fluid dynamics (CFD) tools in recent years, several researchers are involved in studying the hydrodynamics of gas-solid systems, which would be useful in the design, optimization and scale-up process. The detailed predictive simulations using CFD make modeling more accurate and faster. Conventional scaling laws can be used to design a fluidized bed, either larger or smaller, with hydrodynamic similarity. However, similarity of mixing and segregation phenomena is not guaranteed. Hence simulation becomes the only potential tool useful for scaling fluidized beds used for fluidization of multi-component systems.

CHAPTER 2

LITERATURE REVIEW

2. LITERATURE REVIEW:

Most of the gas–solid fluidization behavior studies that have been reported are for cylindrical fluidized beds because of their extensive use in industry, or in rectangular beds for practical experimental reasons. However tapered fluidized beds have many attractive features, among which are their capabilities for handling particles with different sizes and properties (Scott and Hancher, 1976; Ishii *et al.*, 1977) and for achieving extensive particle mixing (Babu et *al.*, 1973). It is reported that the fluidization in tapered beds are more stable compared to that in a cylindrical fluidized bed. Ridgeway has discussed the factors governing the degree of tapering required together with improvement obtained and presented equations to find out the degree of tapering under constant velocity and constant drag conditions. Toyohara and Kawamura (1989) have reported the flow regime of partial fluidization and pressure drop characteristics in gas solid tapered beds of apex angles 30^0 and 45^0, consisting of single size particles of glass beads ranging from 274μm to 650μm. The model developed by Shi et al. is based on Ergun's equation and neglects friction between the particles and the wall. Biswal et al. developed theoretical models, for minimum fluidization velocity and pressure drop in a packed bed of spherical particles for gas–solid systems in conical vessels. Agarwal and Roy have derived equation for prediction of pressure drop at critical fluidization velocity for gas-solid fluidized beds. The equation is tested for air-glass beads, air-urea and air-mustard seeds systems in cones of apex angles of 12.5^0, 14.6^0 and 18.6^0. Maruyama and Koyanagi have studied bed expansion ratio of Geldart D particles using tapered vessels of apex angles ranging from 3.82^0 to 45.24^0 and proposed an equation for bed expansion ratio.

Olazer et al. compared their experimental results with that calculated using the models developed by Gelperin etal.[4] and Gorshtein and Mukhlenov for maximum pressure drop and found that the predictions were not very accurate. They therefore proposed a modified

equation for calculation of maximum pressure drop. Later, Peng and Fan made an in-depth study of the hydrodynamic characteristics of solid–liquid fluidization in a tapered bed and derived theoretical models for the prediction of minimum fluidization velocity and maximum pressure drop, based on the dynamic balance of forces exerted on the particle. The experiments were however carried out for spherical particles only. Jing et al and Shan et al. developed models for gas–solid conical fluidized beds for spherical coarse and fine particles based on the Peng and Fan models but neglected the pressure drop due to the kinetic change in the bed. Depypere et al. have carried out studies in a tapered fluidized bed reactor and proposed empirical models for determination of expanded bed height by using static pressure and wall surface temperature measurements.

Kumar et al [1981] and Yogesh Chandra and Jagannath Rao[1981] have investigated the hydro dynamics of gas -solid fluidization in tapered vessels using single size particles. Some of the previous investigations also include studies on pressure drop of fixed and fluidized beds in tapered vessels (Koloini and Farkas, 1973; Biswal *et al.*, 1984), flow regimes, incipient condition of fluidization, voidage distribution and bed expansion (Hsu, 1978), and particle mixing (Ridgway, 1965; Maruyama and Sato, 199l). The incipient condition of fluidization in a tapered bed can be predicted based on the dynamic balance of forces exerted on the particle bed. This approach was adopted by Gelperin *et al.* (1960) and Nishi (1979) for gas-solid tapered beds, and Shi *et al.* (1984) for liquid-solid tapered beds. Nevertheless, none of these works took into account the phenomenon of partial fluidization in predicting the incipient condition of fluidization and the concomitant, maximum pressure drop. Biswal et al have proposed correlation for fluctuation ratio using glass beads in a cone of apex angle 10^0. Maruyama and Koyanagi have obtained an equation for fluctuation ratio in slugging fluidized beds in the slow bubble regime. Due to angled wall, random and unrestricted particle movement occurs in tapered bed thereby reducing back mixing (Singh et al, 1992). The

hydrodynamic behaviour of binary fluidized beds is strongly influenced by the differences in properties of the respective particles, the availability of internals and the prevailing fluidization regime. S.H. Schaafsma, T. Marks and A.C. Hoffmann have investigated the particle flow pattern and segregation in tapered fluidized bed granulators using segregation experiments and positron emission particle tracking experiments. DiFelice et al have examined the effects of taper on the steady state expansion characteristics of a homogenous fluidized bed. It was shown that secondary factors that might be thought to influence the expansion (fluid accelerational effects including added mass and particle phase elasticity) are unlikely to be of significance in practical situations.

The mixing and segregation in classical and tapered fluidized beds is reported by G. Kwant, W. Prins and W.P.M. van Swaaij (1994). This is based mainly on the reviews by Rowe, Nienow and Chiba.

It is well known that mixing degree of solids in a binary fluidized bed with a constant cross section is always between two extremes, i.e. complete separation and complete mixing of the solid phases. Completely separated binary fluidized beds consist of two distinct fluidized layers, each containing one type of particle only. Conversely, particles of each type are distributed uniformly over the entire solid phase volume in well mixed beds.

The new visual observation of the formation of segregation patterns in fluidized binary systems have been reported by M.A. Gilbertion and I. Eames (2001). It has been shown that a bed consisting of a mixture of particles of different sizes can have a variety of different structures depending on the gas flow rate through it. Their effect on the particles differs according to the local proportions of each component of mixture. Segregation can persist when the gas flow rate is sufficiently large to fluidize the entire bed. Under such conditions it can be shown that the segregation can be successfully modeled by drawing an

analogy with the sedimentation of particles from a turbulent flow field. The experimental results suggest that the efficiency of mixing by the bubbles in a fluidized bed is very much less than for gas bubbles in a liquid.

For segregating fluidized bed (J.M. Beeckmans and R. Agarwal, 1994) the concentration of jetsam in the upper stratum of a strongly segregating bed at steady state is determined solely by the depth of the jetsam layer, the fluidization velocity and the particle properties, especially the minimum fluidization velocities of the two components. A correlation based on the independent variables mentioned as $h = \frac{(1-x)m_j - xm_f}{A(1-\varepsilon)(1-x)\rho_j}$ where m_j is the mass of jetsam in the bed and m_f is the mass of floatsam in the bed.

Sun and Battaglia (2006) performed simulations with and without particle rotation to study segregation phenomena in a bi-dispersed bubbling gas-fluidized bed using a multi-fluid Eulerian model. They claimed that with particle rotation in the kinetic theory model and slightly friction considered the multi-fluid model better captures the bubble dynamics and time-averaged bed behavior. Feng et al. (2004) simulated the flow behavior of flotsam and jetsam particles and found that the degree and rate of segregation or mixing are significantly affected by gas velocity and the final equilibrium states are not affected by the initial packing states for a given gas velocity. The particle segregation occurs as a result of the fluid–particle drag force and the particle–particle interactions.

Continuum two- and multi-fluid model development toward understanding gas–solid flow has been taken place through the development of kinetic theory of granular flow based on the theory for non-uniform dense gases described by Chapman and Cowling (1970). Savage and Jeffrey (1981) showed that dense-phase kinetic theory can be applied to granular flow of particles. They used the term granular temperature to quantify the fluctuating motion of

particles. Kinetic theory of granular particle was developed and applied to predict gas–solid bubbling fluidized beds (e.g., Ding and Gidaspow, 1990; Peirano et al., 2002; Patil et al., 2005). In these models, particles were assumed to be identical spheres. In an actual situation, solid particles may have a wide distribution in sizes and densities. To model fluidization behavior of these particles in a fluidized bed, a multi-particle phase flow model is required. Jenkins and Mancini (1989) have proposed a model for the binary mixture of particles. They assumed that two species of particles in the mixture have the same granular temperature, which is a measure of the average fluctuating energy. Such an assumption can only be held for molecular systems when dissipative effects are absent and the mass ratio of the respective particles is moderate. For multi-particulate phase, this assumption is inappropriate due to the dissipation associated with the inelasticity of particle–particle collisions. Gidaspow et al. (1996) extended the kinetic theory of dense gases to binary granular mixture with unequal granular temperatures. Recently, many activities on computational fluid dynamics (CFD) modeling of fluidizations with mixture particles have been conducted. Mathiesen et al. (1999) predicted the axial and radial velocities and volume fractions for two different sizes of particles in a CFB riser. Goldschmidt et al. (2001) studied the effect of coefficient of restitution on the segregation behavior in dense gas-fluidized beds based on a multi-fluid model. Van Wachem et al. (2001) predicted the flow behavior of gas-fluidized bed with a bimodal particle mixture model. Some of the problems with respect to CFD model validation for gas–solid systems have been reviewed by Grace and Taghipour (2004). Taghipour et al. (2005) presented CFD simulation of two-dimensional (2D) cylindrical columns and observed that the motion of bubbles and particles are greatly influenced by the wall effect in a 2D column. Recently detail CFD simulation of conical spouted bed has been carried out by Wang Z. (2006).

S. Cooper and C.J. Coronella have done CFD simulations of particle mixing in a binary fluidized bed using coke and rutile, with different diameters and densities. Simulation was done using FLUENT^{TM} 6.0.

Though, there has been an increased research activity in the use of tapered fluidized beds, most of the works are limited to hydrodynamic studies of single particle system or binary mixtures. In light of the literature survey, it may be stated that the study of mixing and segregation characteristics is done extensively for cylindrical beds but no detailed work has been reported on the study of mixing and segregation processes in tapered fluidized beds. The high potential of industrial-scale applications of mixing and segregation processes has acted as a driving force for investigations required to make the efficiency of this process really attractive.

CHAPTER 3

MIXING AND SEGREGATION

3. MIXING AND SEGREGATION:

Bubbling fluidized beds undergo extensive particle mixing, due to the motion of the bubbles themselves. However, under certain cooperating conditions, segregation may take place. Either mixing or segregation may be desirable, depending upon the applications of the fluidized bed. Mixing, for instance, is more important in gas-solid contact reactors. The rapid mixing of solids in fluidized beds leads to close to isothermal conditions throughout the reactor; so the control of the operation becomes more reliable. However, segregation is more important in classifiers where solids are to be separated based on size or density.

3.1. MECHANISM OF MIXING AND SEGREGATION:

The upward motion of bubbles through the bed of solids determines both the mixing and the segregation of particles, and is in accord with the two-phase theory of fluidization. As the bubble travels up through the bed, particles are drawn into a stagnant zone trailing the bubble called the wake. Axial mixing occurs as particles slough off the wake and new particles enter from the dense surrounding region. When the bubble reaches the top of the bed, the particles from the wake are deposited at the surface. By this mechanism, particles from the bottom of the bed may be mixed with those at the top. Meanwhile, the rising bubble leaves a void as it moves. This void is filled by particles falling down around the bubble. Those particles that tend to segregate to the bottom tend to fall just a little further and are referred to as jetsam. Particles that tend to accumulate at the top of the bed are called flotsam and fall less quickly. Mixing and segregation occur simultaneously, and at equilibrium the result of these processes is a concentration gradient in the axial direction while maintaining a fairly uniform distribution of particles radially.

Solids that have a wide particle-size distribution have been shown to exhibit segregation due to differences in drag per unit weight. Particles of equal density exhibiting a higher drag per

unit weight tend to behave as flotsam, while those with lower drag are jetsam. Generally, this results in larger particles accumulating at the bottom of the bed. However, particles of different densities are more likely to segregate than in systems with a wide size distribution.

3.2. VARIABLES EFFECTING MIXING AND SEGREGATION:

From a practical point of view, a gas fluidized bed is usually assumed to be well mixed. However, segregation may occur when the bed contains more than one type /size of material. In that case, segregation will take place due to the differences in particle properties, such as particles densities size and shape. In general, segregation is more influenced by density difference. One of the main cause of the segregation is force imbalances on particles during the periodic disturbances (due to the density differences) associated with passage of the bubbles [06]. Further more other parameters that determine the extent of particle segregation in a fluidized bed system is related to the amount of particles used.The characteristic parameter in this case is as follows:

1. The bed aspect ratio (H/Dc) at minimum fluidization, which is related to the total amount bed material.
2. The weight ratio of the segregating components in the bed
3. The Critical bed diameter(At which value the segregation is nil)
4. The properties of the fluidized bed system which are independent of particle properties. These include

(a) Fluidized bed dimension, such as the bed diameter and the height.

(b) The bed operating conditions such as superficial gas velocities.

(c) Position baffled, distributor and hole diameter and pitch and opening ratio of holes on the baffles as well as distributors.

CHAPTER 4

COMPUTATIONAL FLUID DYNAMICS

4. COMPUTATIONAL FLUID DYNAMICS (CFD) :

CFD is one of the branches of fluid mechanics that uses numerical methods and algorithms to solve and analyze problems that involve fluid flows. Computers are used to perform the millions of calculations required to simulate the interaction of fluids and gases with the complex surfaces used in engineering. However, even with simplified equations and high speed supercomputers, only approximate solutions can be achieved in many cases. More accurate codes that can accurately and quickly simulate even complex scenarios such as supersonic or turbulent flows are an ongoing area of research.

4.1. BACKGROUND

The fundamental basis of any CFD problem is the Navier-Stokes equations, which define any single-phase fluid flow. These equations can be simplified by removing terms describing viscosity to yield the Euler equations. Further simplification, by removing terms describing vorticity yields the Full Potential equations. Finally, these equations can be linearized to yield the Linearized Potential equations.

CFD techniques is now a promising tool to model fluidized bed dynamics due to it's many advantages such as design, optimization and scale-up of processes. Johansson et al. (2006) simulated conventional fluidized beds using two different closure models for the particle phase stresses. The first one uses a constant particle viscosity (CPV) and predicts particle pressure. The second approach uses the particle turbulence model (PT) which is also known as granular temperature model (Enwald et al.,1999). This model is based on kinetic theory of granular flow (KTGF) and derived in analogy with the kinetic theory of gases (Lun et al., 1984). The solid particles are generally considered to be identical. Johansson et al. (2006) also reported that the KTGF model results are in better agreement with the experiments.

The two common approaches for modeling gas-solid fluidized beds are Eulerian-Lagrangian model, where the gas is treated as the continuous phase and the solid as the discrete phase, and the Eulerian-Eulerian model, where the two phases are treated as interpenetrating continua. Where the solids is treated as discrete, the particle trajectory is obtained by solving the Newton's equation of motion taking into account the collision between the particles and the force exerted on the particles by the gas. The transport coefficients of the solid phases also include gas–particle interactions and particle–particle collisions terms. For the resultant continuum approximation, certain averaging techniques and assumptions are required to obtain a momentum balance for the solids phase.

4.2. METHODOLOGY:

In all of these approaches the same basic procedure is followed.

1. The geometry (physical bounds) of the problem is defined.
2. The volume occupied by the fluid is divided into discrete cells (the mesh).
3. The physical modelling is defined - for example, the equations of motions + enthalpy + species conservation
4. Boundary conditions are defined. This involves specifying the fluid behaviour and properties at the boundaries of the problem. For transient problems, the initial conditions are also defined.
5. The equations are solved iteratively as a steady-state or transient.
6. Analysis and visualization of the resulting solution.

4.3. GAMBIT (CFD PREPROCESSOR)

It is a software package designed to help analyst and designers build and mesh models for CFD and other scientific applications.

The Gambit graphical user interface makes the basic steps of:

- Building.
- Meshing,
- Assigning zones type to a model

Gambit has following advantages:

1. **Ease of use:** It is user friendly
2. **CAD/CAE Integration:** Gambit can import geometry from any CAD/CAE software
3. **Fast Modeling:** It provides a concise and powerful set of solid modeling based geometry tools
4. **CAD cleanup:** Gambit's semiautomatic cleanup tools can be used to repair and prepare the geometry for high quality meshing.
5. **Intelligent Meshing:** Different CFD problems require different mesh types.

Gambit provides a wide variety of meshing tools.

Step 1: Building the geometry

There are two approaches to build the geometry

- **Top Down:** Construct the geometry by creating volumes (bricks, cylinder etc) and then multiplying them through boolean operation.
- **Bottom Up:** Create vertices, then creating edges from vertices, then connect the edges to create faces and then connect the faces to create volume.

Step 2: Meshing the model

Meshing can be done in different ways:

→ Triangular, quadrilateral, hexahedral, tetrahedral, prism etc.

→ Structured and unstructured mesh.

Step 3: Specifying zones type

Zone type specification defines the physical and operational characteristics of the model at its boundaries and within specific region of its domain. There are two classes of zone type specification

- **Boundary type:** In this type specifications, such as well, vent or inlet, define the characteristics of the model at its external or internal boundaries.
- **Continuum type:** In this type specification, such as fluid or solid, define the characteristics of the model within specified regions of its domain. e.g. if you assign a fluid continuum type specification to a volume entity, the model is defined such that equations of momentum, continuity and species transport apply at mesh nodes or cells that exist within the volume. Conversely if you assign a solid continuum type specification to a volume entity, only the energy and species transport equations (without convection) apply at the mesh nodes or cells that exist within the volume.

  Fluid zone = group of cells for which all active equations are solved.

  Solid zone = group of cells for which only heat conduction problem solved.
  No flow equations solved.

5. HOW DOES A CFD CODE WORK?

CFD codes are structured around the numerical algorithms that can be tackle fluid flow problems. In order to provide easy access to their solving power all commercial CFD packages include sophisticated user interfaces input problem parameters and to examine the results. Hence all codes contain three main elements:

1. Pre-processing.
2. Solver
3. Post –processing.

4.4.1. Pre-Processing:

Preprocessor consist of input of a flow problem by means of an operator friendly interface and subsequent transformation of this input into form of suitable for the use by the solver.

The user activities at the Pre-processing stage involve:

• Definition of the geometry of the region: The computational domain.

• Grid generation the subdivision of the domain into a number of smaller, non-overlapping sub domains (or control volumes or elements Selection of physical or chemical phenomena that need to be modeled).

• Definition of fluid properties

• Specification of appropriate boundary conditions at cells, which coincide with or touch the boundary.

The solution of a flow problem (velocity, pressure, temperature etc.) is defined at odes inside each cell. The accuracy of CFD solutions is governed by number of cells in the grid. In general, the larger number of cells betters the solution accuracy. Both the accuracy of the solution & its cost in terms of necessary computer hardware & calculation time are

dependent on the fineness of the grid. Efforts are underway to develop CFD codes with a (self) adaptive meshing capability.

Ultimately such programs will automatically refine the grid in areas of rapid variation.

4.4.2. Solver:

These are three distinct streams of numerical solutions techniques: finite difference, finite volume& finite element methods. In outline the numerical methods that form the basis of solver performs the following steps

- Approximation of unknown flow variables by means of simple functions.
- Discretization by substitution of the approximation into the governing flow equations & subsequent mathematical manipulations.
- Solution of the algebraic equations.

4.4.3. Post-Processing:

As in the pre-processing huge amount of development work has recently has taken place in the post processing field. Owing to increased popularity of engineering work stations, many of which has outstanding graphics capabilities, the leading CFD are now equipped with versatile data visualization tools. These include

- Ø Domain geometry & Grid display.
- Ø Vector plots.
- Ø Line & shaded contour plots.
- Ø 2D & 3D surface plots.
- Ø Particle tracking.
- Ø View manipulation (translation, rotation, scaling etc.)

4.5. ADVANTAGES OF CFD:

Major advancements in the area of gas-solid multiphase flow modeling offer substantial process improvements that have the potential to significantly improve process plant operations. Prediction of gas solid flow fields, in processes such as pneumatic transport lines, risers, fluidized bed reactors, hoppers and precipitators are crucial to the operation of most process plants. Up to now, the inability to accurately model these interactions has limited the role that simulation could play in improving operations. In recent years, computational fluid dynamics (CFD) software developers have focused on this area to develop new modeling methods that can simulate gas-liquid-solid flows to a much higher level of reliability. As a result, process industry engineers are beginning to utilize these methods to make major improvements by evaluating alternatives that would be, if not impossible, too expensive or time-consuming to trial on the plant floor. Over the past few decades, CFD has been used to improve process design by allowing engineers to simulate the performance of alternative configurations, eliminating guesswork that would normally be used to establish equipment geometry and process conditions. The use of CFD enables engineers to obtain solutions for problems with complex geometry and boundary conditions. A CFD analysis yields values for pressure, fluid velocity, temperature, and species or phase concentration on a computational grid throughout the solution domain.

The key advantages of CFD are:

1. It provides the flexibility to change design parameters without the expense of hardware changes. Hence it costs less than laboratory or field experiments, allowing engineers to try more alternative designs than would be feasible otherwise.

2. It has a faster turnaround time than experiments.

3. It guides the engineer to the root of problems, and is therefore well suited for trouble-shooting.

4. It provides comprehensive information about a flow field, especially in regions where measurements are either difficult or impossible to obtain.

CHAPTER 5

EXPERIMENTAL SECTION

5. EXPERIMENTAL SECTION:

5.1. EXPERIMENTAL SET UP:

5.1.1. SCHEMATIC DIAGRAM:

The schematic diagram of experimental setup is shown below.

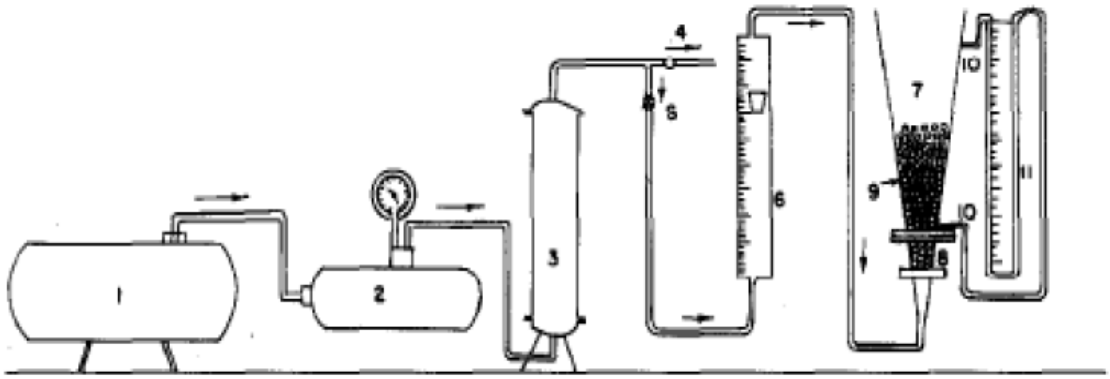

1. Compressor, 2. Receiver, 3. Silica-gel Tower, 4. By pass valve, 5. Line Valve, 6. Rotameter, 7. Conical Fluidizer, 8. Glass beads packing 9. Glass beads in fluidized state, 10. Pressure tapings to manometer

Fig. 4.1 Schematic diagram of experimental set up

5.1.2. CONSTITUENTS OF EXPERIMENTAL SETUP:

The experimental set up consists of the following parts

5.1.2.1.Air Compressor:

It is a multistage air compressor of sufficient capacity.

5.1.2.2.Air Receiver:

It is a horizontal cylinder used for storing the compressed air from compressor. There is one G.I. pipe inlet to the receiver and one by-pass from one end of the cylinder. The exit line is also a G.I line taken from the central part of the cylinder. The purpose for using air accumulator in the line is to dampen the pressure fluctuations. The accumulator is fitted with a pressure gauge. The operating pressure in the cylinder is kept at 20psig**.**

5.1.2.3.Silica-Gel Column:

A silica gel column is provided in the line immediately after the air receiver to arrest the moisture carried by air from the receiver.

5.1.2.4.Pressure Gauge:

A pressure gauge, in the required range (1-50psig.), is fitted in the line for monitoring the working pressure.

5.1.2.5.Rotameter:

Rotameter is used for the measurement of flow rate of air. Two rotameters, one for the lower range (0-20 m^3/hr) and the other for the higher range (20-120 m^3/hr) were used to measure the air flow rates.

5.1.2.6.Air Distributor :

Air distributor is a perforated plate made up of G.I sheet. The pores of 0.5cm diameter are randomly placed on the sheet. The distributor is an integral part of calming section where it is followed by a conical section. The inside hollow space of the distributor is filled with glass beads of 1.5cm outer diameter, for uniform air distribution**.**

5.1.2.7.Conical Fluidizer :

The fluidizer consists of transport Perspex column with one end fixed to flange. The flange has 6 bolt holes of 1.2 cm. diameter. Two pressure tapings are provided for noting the bed pressure drop. A screen is provided in the lower flange of the fluidizer and the conical air distributor.

5.1.2.8.Quick Opening Valve And Control Valve:

A globe valve of 1.25cm inner diameter is attached next to the pressure gauge for sudden release of the line pressure. A gate valve of 15mm inner diameter is provided in the line to control the airflow to the bed.

5.1.2.9.Manometer Panel Board:

One set of manometers is arranged in the panel board to measure the pressure drop. Carbon tetrachloride is used as manometric fluid.

5.1.2.10.Vacuum Pump:

The vacuum pump is used to draw the material from the bed during mixing- segregation experiments.

5.1.3. STRUCTURE OF TAPERED BED:

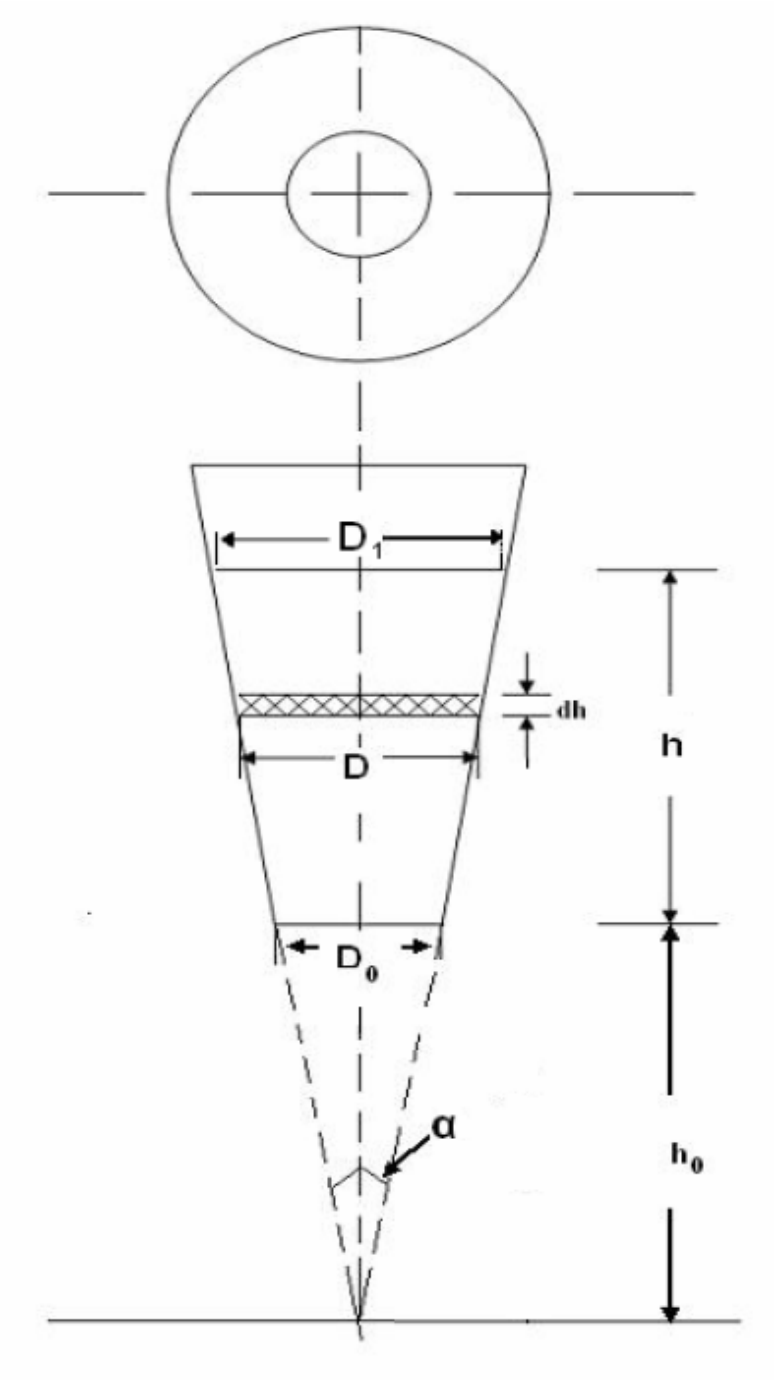

Fig. 4.2 Structure of tapered bed

5.1.4. APPARATUS DATA:

The tapered column was made of Perspex sheets to allow visual observation. The inlet diameter was 45mm where as the outlet diameter was177 mm. The reactor height is 545 mm. The tapered angle is 6.9º. A 60 mesh screen at the bottom served as the support as well as the distributor. The calming section of the bed was filled with glass beads for uniform distribution of fluid. Two pressure taps, one at the entrance and the other at the exit section of the bed were provided to record the pressure drops. Pressure drop was measured by manometer, which was one meter long. Carbon tetrachloride (density=1594 kg m^{-3}) was used as the manometric fluid. Air at a temperature of 28 ^{0}C (ρ=1.17 kg m^{-3} and μ=1.8*10^{-5} kg m^{-1} s^{-1}) used as the fluidizing medium was passed through a receiver and a silica gel tower to dry and control the air flow before being sent through the tapered column. Two rotameters, one for the lower range (0-20 m^{3}/hr) and the other for the higher range (20-120 m^{3}/hr) were used to measure the air flow rates. The vacuum pump is used to draw the material from the bed during mixing- segregation experiments

5.2. EXPERIMENTAL PROCEDURE:

5.2.1. HYDRODYNAMIC STUDIES:

A weighed amount of material was charged to the bed. The initial stagnant bed height was recorded. Then the air flow rate was increased incrementally allowing sufficient time to reach a steady state. The rotameter and manometer readings were noted for each increment in flow rate and the pressure drop and superficial velocity calculated. When the minimum fluidization was attained, the expanded static bed height was also measured. As the bed fluctuates between two limits of gas-solid fluidization, heights of the upper and the lower surfaces of the fluctuating bed were measured for each fluid velocity higher than the minimum fluidization velocity.

5.2.2. MIXING-SEGRAGATION EXPERIMENTS:

After fluidizing the bed with a particular fluid mass velocity, it was brought to static condition by closing the air supply. The bed was then divided into different layers each of two cm height. Each of the layers was drawn applying suction and analyzed for the amount of jetsam particles present. Such a system was referred as the static bed condition.

5.3. CFD ANALYSIS USING FLUENT 6.2:

5.3.1. GRID AND MESH:

The simulated bubbling fluidized bed is a tapered bed with an inlet diameter of 45mm where as the outlet diameter was 177 mm. The reactor height is 545 mm.. A two-dimensional grid was created in a CAD program called GAMBIT 2.0.30 and exported into FLUENT™ 6.2.16.

The simulated bed contains a gas jet on the bottom of the bed. Along the horizontal and vertical directions, the grid size is 0.001mm, resulting in a total of 85491 cells. This grid was created to simulate the gas flow patterns observed in the laboratory-scale bed.

Additionally, the grid is divided into a lower zone and an upper zone for the purpose of specifying initial conditions. At time zero, the lower zone is filled with solids at an appropriate volume fraction, while the upper zone contains no solids initially.

5.3.2. THE SOLVER:

In order to model the transient nature of a bubbling fluidized bed, a non-steady state, Eulerian multiphase model is used. The following assumptions have been taken during the formation and simulation of tapered bed:

- Ø No mass transfer is allowed between the gas phase and the solid phase
- Ø External body force, lift force, as well as virtual mass force is ignored

- Ø Pressure gradient at full fluidization is constant
- Ø Density of each phase is assumed to be constant

Based on the general description of the Eulerian multiphase model and the above assumptions, the following governing equations can be derived for gas-solid flow systems.

5.3.2.1. Conservation equations of mass and momentum:

The well-known continuity equation, or mass balance for phase i (gas or solid) with temporal and spatial gradients is given as:

$$\frac{\partial}{\partial t}\left(\varepsilon_i.\rho_i\right)+\nabla.\left(\varepsilon_i.\rho_i.\vec{v}_i\right)=0 \qquad (5.1)$$

$$\varepsilon_g+\varepsilon_s=1 \qquad (5.2)$$

The momentum balance for the gas phase given by the Navier-Stokes equation is modified to include an interphase momentum transfer term and a solid phase source term:

$$\frac{\partial}{\partial t}.\left(\varepsilon_g.\rho_g.\vec{v}_g\right)+\nabla.\left(\varepsilon_g.\rho_g.\vec{v}_g^{\,2}\right)=-\varepsilon_g.\nabla P+\varepsilon_g\nabla.\bar{\bar{\tau}}_g+\varepsilon_g.\rho_g.\vec{g}-K_{gs}.\left(\vec{v}_g-\vec{v}_s\right) \qquad (5.3)$$

$$\frac{\partial}{\partial t}.\left(\varepsilon_s.\rho_s.\vec{v}_s\right)+\nabla.\left(\varepsilon_s.\rho_s.\vec{v}_s^{\,2}\right)=-\varepsilon_s.\nabla P-\nabla P_s+\nabla.\bar{\bar{\tau}}_s+\varepsilon_s.\rho_s.\vec{g}+K_{gs}.\left(\vec{v}_g-\vec{v}_s\right)+\vec{S}_s \qquad (5.4)$$

where, the left hand side (LHS) represents the temporal and spatial transport terms and the right hand side (RHS) represents the various interacting forces. The first term on the RHS of Equations. 5.3 and 5.4 represents the hydrodynamic pressure due to the gas and solid phases, respectively. The second term of Eq^{n} 5.4 accounts for the normal stresses developed due to the collision between the solid particles. The second term on RHS of Eq^{n} 5.3 and the third term on RHS of Eq^{n} 5.4 account for the gas shear stress and the solid shear stress due to collision of solid particles, respectively. The fourth term on RHS of Eq^{n} 5.3 and fifth term on RHS of Eq^{n} 5.4 represent the momentum exchange between the solids and the gas phase. The

last term on RHS of Eq^{n} 5.4 represents the source term which accounts for all other forces that may affect the flow.

5.3.2.2. Kinetic theory of granular flow equations:

In order to solve Eq^{n}s 5.3 and 5.4, it is necessary to have closure equations to relate the unknowns in these equations. The solid phase is treated as pseudo-homogenous, and in the present study the kinetic theory of granular flow developed by Lun et al. (1984) was used to define the solid phase properties.

Analogous to the thermodynamic temperature for gases, the granular temperature Θ_s can be introduced as a measure of the particle velocity fluctuation, i.e.,

$$\Theta_s = \frac{1}{3}\left(v_s'^2\right) \tag{5.5}$$

The transport equation for the fluctuating kinetic energy for the granular phase as given by Chapman and Cowling (1990) is

$$\frac{3}{2}.\left[\frac{\partial}{\partial t}.\left(\rho_s.\varepsilon_s.\Theta_s\right)+\nabla.\left(\rho_s.\varepsilon_s.\underline{v}_s.\Theta_s\right)\right]=\left(-p_s\bar{\bar{I}}+\bar{\bar{\tau}}_s\right):\nabla.\underline{v}_s+\nabla.\left(k_{\Theta s}.\nabla.\Theta_s\right)-\gamma_{\Theta s}+\phi_{is} \tag{5.6}$$

where $\left(-p_s\bar{\bar{I}}+\bar{\bar{\tau}}_s\right):\nabla.\underline{v}_s$ is the generation of energy by the solid stress tensor because of the interaction between the normal and shear stress matrix with the mean velocity field, $k_{\Theta s}\nabla\Theta_s$ accounts for the transport of energy due to diffusion ($k_{\Theta s}$ is the diffusion coefficient), $\gamma_{\Theta s}$ is the dissipation of energy due to collision and is given as,

$$\gamma_{\Theta s} = ((12(1-e_{ss}^{\ 2})g_{0,ss})/d_s\sqrt{\pi})\rho_s\varepsilon_s^{\ 2}\Theta_s^{\frac{3}{2}}.$$

The last term on the RHS is the exchange of kinetic energy between the solid and the gas phases, given as,

$$\phi_{gs} = -3k_{gs}\Theta_s$$

The stress-strain tensor for phase i is given as,

$$\overline{\overline{\tau}}_i = \varepsilon_i \mu_i \left(\nabla \vec{v}_i + \nabla \vec{v}_i^T \right) + \varepsilon_i \left(\lambda_i - \frac{2}{3}\mu_i \right) \nabla \cdot \vec{v}_i \overline{\overline{I}} \tag{5.7}$$

For the solid phase, s, the solids shear viscosity is the sum of the collisional viscosity, kinetic viscosity and optional frictional viscosity and is given as

$$\mu_s = \mu_{s,col} + \mu_{s,kin} + \mu_{s,fr} \tag{5.8}$$

The collision viscosity is given as,

$$\mu_{s,col} = \frac{4}{5}\varepsilon_s \rho_s d_s g_{0,ss}\left(1+e_{ss}\right)\left(\frac{\Theta_s}{\pi}\right)^{1/2} \tag{5.9}$$

where $g_{0,ss}$ is defined as,

$$g_{0,ss} = \left[1-\left(\frac{\varepsilon_s}{\varepsilon_{s,max}}\right)^{1/3}\right]^{-1} \tag{5.10}$$

The following expression from Gidaspow (1994) was used to estimate the kinetic viscosity.

$$\mu_{s,kin} = \frac{10\rho_s d_s \sqrt{\Theta_s \pi}}{96\varepsilon_s\left(1+e_{ss}\right)g_{0,ss}}\left[1+\frac{4}{5}g_{0,ss}\varepsilon_s\left(1+e_{ss}\right)\right]^2 \tag{5.11}$$

The solid bulk viscosity as given by Lun et al. (1984) is,

$$\lambda_s = \frac{4}{3}\varepsilon_s \rho_s d_s g_{0,ss}\left(1+e_{ss}\right)\left(\frac{\Theta_s}{\pi}\right)^{1/2} \tag{5.12}$$

The frictional viscosity as defined by Schaeffer (1987) is,

$$\mu_{s,fr} = \frac{P_s \sin(\Phi)}{2\sqrt{I_{2D}}} \tag{5.13}$$

5.3.2.3. Drag model (Fluid –solid exchange coefficients):

The drag force acting on a particle in a fluid-solid system can be represented by the product of a momentum exchange coefficient and the slip velocity between the two phases. The correlations of K_{sg} are usually obtained from pressure drop measurements in fixed, fluidized, or settling beds. For the motion of particle swarms, however, it has been found that the volume fraction of the particle phase has a complex and subtle influence on drag force.

The fluid-solid exchange coefficient K_{sg} can be written in the following general form:

$$K_{sg} = \frac{\varepsilon_s \rho_s f}{\tau_p} \tag{5.14}$$

where f depend on the different exchange coefficient models and τ_p is defined as

$$\tau_p = \frac{\rho_s d_s^{\,2}}{18\mu_g} \tag{5.15}$$

Several models for the fluid-solid exchange coefficient are available in the literature. In the present study, however, the Gidaspow (1994) drag model has been used. The Gidaspow model is a combination of the Wen and Yu (1966) model and the Ergun (1952) equation.

When $\varepsilon_g > 0.8$, the fluid-solid exchange coefficient K_{sg} is of the following form:

$$K_{sg} = \frac{3}{4} C_D \frac{\varepsilon_s \varepsilon_g \rho_g \left| \vec{v}_s - \vec{v}_g \right|}{d_s} \varepsilon_g^{-2.65} \tag{5.16}$$

where,

$$C_D = \frac{24}{\varepsilon_g \,\mathrm{Re}_s} \left[1 + 0.15 \left(\varepsilon_g \,\mathrm{Re}_s \right)^{0.687} \right] \tag{5.17}$$

$$\mathrm{Re}_s = \frac{\rho_g d_s \left| \vec{v}_s - \vec{v}_g \right|}{\mu_g} \tag{5.18}$$

When, $\varepsilon_g \leq 0.8$

$$K_{sg} = 150\frac{\varepsilon_s\left(1-\varepsilon_g\right)\mu_g}{\varepsilon_g {d_s}^2} + 1.75\frac{\rho_g \varepsilon_s \left|\vec{v}_s - \vec{v}_g\right|}{d_s} \tag{5.19}$$

`5.3.3. SOLIDS PRESSURE:

For granular flows in the compressible regime (i.e., where the solids volume fraction is less than its maximum allowed value), a solids pressure is calculated independently and used for the pressure gradient term, ∇P_s, in the solids phase momentum equation. The solids pressure is composed of a kinetic term and a second term due to particle collision. The solid pressure as given by Lun et al. (1984) is,

$$P_s = \varepsilon_s \rho_s \Theta_s + 2\rho_s\left((1+e_{ss})\varepsilon_s^{\,2} g_{0,ss}\Theta_s\right. \tag{5.20}$$

5.3.4. THE SOLID PHASE SOURCE TERM IN TAPERED BEDS:

For tapered beds, there exist three distinct regions: a dilute core, a dense annular region between the core and the wall named the annulus, and a dilute hump region above the bed surface (Peng and Fan, 1997). For simulation of the tapered bed, the bed should be divided mainly two regions: a dilute fluidized region (including both the core and the hump) and a dense defluidized region (annulus). It was found in a tapered bed that the ratio of the maximum pressure drop to the pressure drop at partial fluidization and full fluidization is usually greater than one. To include the stress exerted by the tapered side wall on the gas-solids flow, two solid phase source terms (Wang Z., 2006) are introduced into the core and annulus regions respectively with the following forms:

$$K_a = \frac{\nabla P_{\max}}{\nabla P_{fb}} \tag{5.21}$$

$$K_c = f\left(\varepsilon_{g,0}, \rho_s, d_s, \rho_g, \mu_g, v_{g,z}\right) \tag{5.22}$$

$\nabla P_{\max}$ can be obtained either from experiments or empirical expressions from the literature. Though K_c is a function of different parameters, for simplification of the problem, K_c was assumed to be one. Based on Ergun (1952) and Wen and Yu (1966) drag equations the following simple expressions were used to describe the solid phase source term.

When $\varepsilon_g \le 0.8$ and $Z \le H_0$ (in the annulus),

$$S_{s,a} = -\varepsilon_s \rho_s g + K_a \left(\varepsilon_s \rho_s g\right) = \left(K_a - 1\right)\varepsilon_s \rho_s g \qquad (5.23)$$

When $\varepsilon_g > 0.8$ (in the core and the hump),

$$S_{s,c} = -\varepsilon_s \rho_s g + K_c \left(\varepsilon_s \rho_s g\right) = \left(K_c - 1\right)\varepsilon_s \rho_s g \qquad (5.24)$$

The actual pressure gradient in a tapered bed is the combination of the gravity term and the solid phase source term in the annulus. Different values of K_a (or different solid phase source terms) represent different values of the pressure gradient in a tapered bed. At minimum fluidization condition, K_a is taken as 1.

5.3.5. MATERIAL PROPERTIES:

In order to simplify the physical experiments [35], the system is described by using a single gas phase and two granular phases. Each granular phase has a single density and a single particle size to reduce the computational effort, as additional particle sizes would increase the number of phases and the computational complexity of the problem. The physical properties of both the gas and solid phases are given in Table 1 and Table 2, respectively.

Table 5.1: Material properties of gas phase

Material	Temperature (°C)	Viscosity (kg $m^{-1}s^{-1}$)	Density (kg/m^3)
Air	28	$1.8*10^{-5}$	1.17

Table 5.2: Material properties of solid phases

Material	Density (kg/m^3)
Glass beads	2600
Dolomite	2800

The maximum packing fraction for each solid phase is also specified. If there are multiple solid phases present in the system, FLUENT™ will apply the largest solids packing fraction for all of the solids present.

5.3.6. BOUNDARY CONDITIONS:

The inlet was designated as "Velocity Inlet" in FLUENT™, where the direction of gas flow is normal to the surface. The flow rates used for inlet is determined from the superficial gas velocity required. No solids are introduced through the nozzles. The effects of superficial gas velocity on mixing were investigated by changing this velocity in simulations. The top of the bed was set as a constant pressure outlet, and the walls were all set as no-slip walls.

5.3.7. SOLUTION CONTROL PARAMETERS:

Either a first-order upwind or a second-order discretization may be selected for both momentum and volume-fraction solutions. Discretization is the process by which the governing partial differential equations are converted to algebraic equations for numerical solution. For a first-order upwind solution, the value at the center of a cell is assumed to be an average throughout the cell. On the other hand, a second-order upwind solution uses a gradient from the cell face to the cell center. Additionally, a limiter is used so that new minima or maxima are not created from the discretization process.

For a bubbling fluidized bed, the selection of the discretization method can have a profound effect on behavior of the system. While a first-order method is quicker, the bubbles that are produced in the simulation are not realistic. Systems that are modeled using a first-order discretization scheme exhibit a large initial bubble, followed by much smaller bullet-shaped bubbles. These small bubbles are abnormally pointed on the crown (leading edge) and contain little wake. Additionally, the bubbles do not interact with one another. They exhibit neither splitting nor coalescence. Bubbles simulated in a solution using a second-order discretization technique are more realistic in shape and behavior. The drastic difference between the two methods has been attributed to numerical diffusion in first-order solutions of the solids' momentum equations.

5.3.8. INITIALIZATION:

The initial bed of solids is packed into the bottom of the bed. The initial concentrations of materials of both sizes are based upon the maximum packing fraction for the materials. The specified volume fraction of solids in the bed is initially 0.01 less than the maximum solids packing fraction. If the initial solids fraction is too high, then convergence problems will occur. If the initial solids fraction is much smaller than the maximum packing fraction, then settling will occur before fluidization. The initial condition patched (specified) was that of perfectly mixed solids throughout.

5.3.9. ITERATIONS:

A time step of 0.001s to 0.0002s with 20 iterations per time step was chosen. This iteration was adequate to achieve convergence for the majority of time steps. The relative error between two successive iterations was specified by using a convergence criterion of 0.001 for each scaled residual component. The pressure–velocity coupling is obtained by phase-coupled SIMPLEX algorithm.

CHAPTER 6

RESULTS AND DISCUSSION

6. RESULTS AND DISCUSSION:

6.1. FLUIDIZATION USING DIFFERENT MATERIALS:

Table 6.1:

Glass beads (Size:BSS -8+12, Bed height=9.8cm, mass =300gm)

$Q(m^3/hr)$	P(cm)	$P(N/m^2)$	U(m/s)
0	0	0.00	0.00
10	5	781.00	1.75
12	8.4	1313.52	2.10
14	11.2	1751.36	2.45
16	8.4	1313.52	2.80
18	8.3	1297.88	3.14
20	8.1	1266.61	3.49
22	8	1250.97	3.84
24	7.9	1235.33	4.19
26	7.6	1188.42	4.54
28	7.6	1188.42	4.89

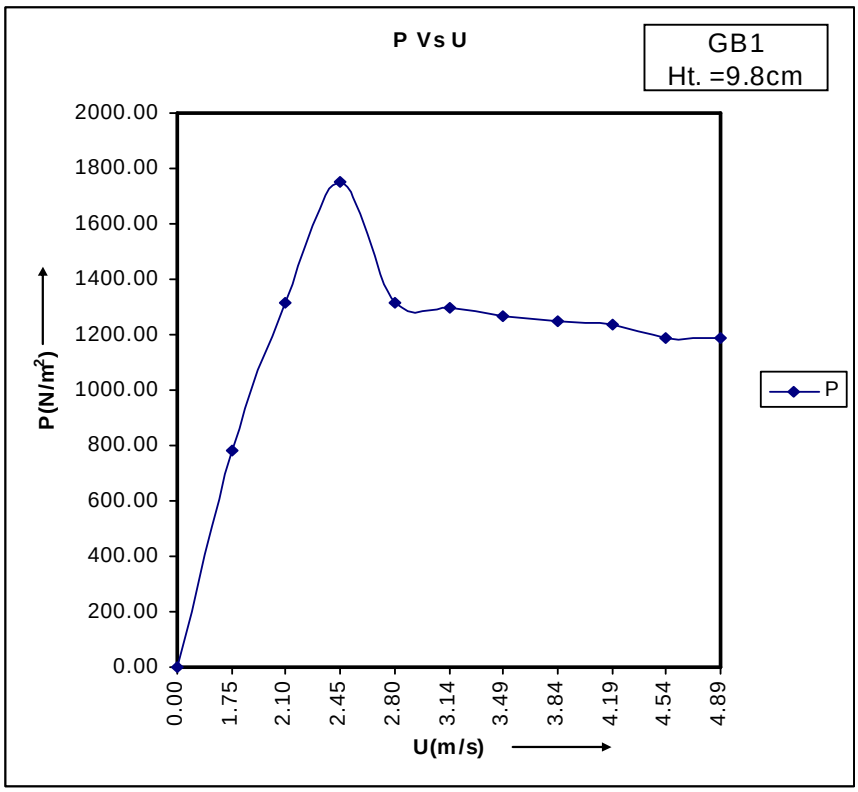

Fig.6.1 ΔP Vs U plot for glass beads of -8+12 mesh size

Table 6.2:

Glass beads (Size:BSS -8+12, Bed height=13cm, mass =485gm)

$Q(m^3/hr)$	U(m/s)	P(cm)	$P(N/m^2)$
0	0	0	0
5.5	0.96	9.5	1483.90
6	1.05	10.9	1702.58
7.5	1.31	14.6	2280.52
8	1.40	17.8	2780.36
8.5	1.48	13.5	2108.70
9	1.57	13.4	2093.08
9.5	1.66	13.2	2061.84
10.25	1.79	13.2	2061.84
13.25	2.31	13.4	2093.08
14.5	2.53	13.6	2124.32
14.75	2.58	12.5	1952.50
16.25	2.84	12.5	1952.50
17	2.97	13	2030.60
17.75	3.10	12.6	1968.12
19	3.32	12.5	1952.50
19.75	3.45	12.3	1921.26

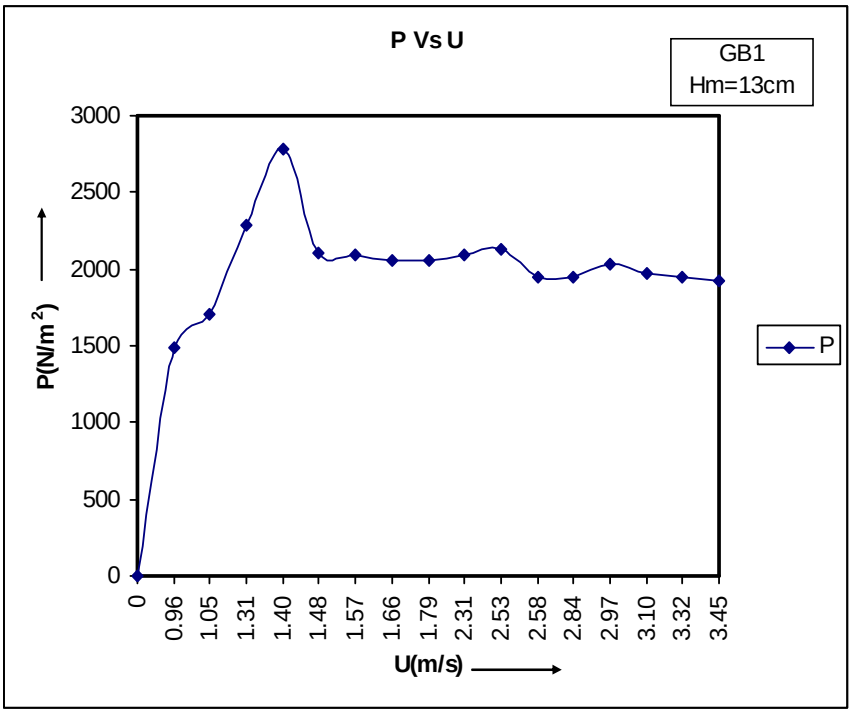

Fig. 6.2 ΔP Vs U plot for glass beads of -8+12 mesh size

Table 6.3:

Glass beads (Size: BSS -8+12 (50%) and BSS -12+14 (50%), Bed height=13cm)

$Q(m^3/hr)$	U(m/s)	P(cm)	$P(N/m^2)$
0	0	0	0
5.5	0.96	8.5	1327.70
6	1.05	10.5	1640.10
6.5	1.14	14.9	2327.38
7	1.22	18.2	2842.84
8	1.40	12.8	1999.36
8.75	1.53	12.6	1968.12
9.5	1.66	12.9	2014.98
10.5	1.83	12.4	1936.88
12	2.10	12.1	1890.02
12.5	2.18	12	1874.40
13.5	2.36	12.1	1890.02
14	2.45	12.2	1905.64
15	2.62	12.5	1952.50
16	2.80	12.4	1936.88
16.75	2.93	12.3	1921.26
17.75	3.10	12.3	1921.26
19	3.32	12.5	1952.50

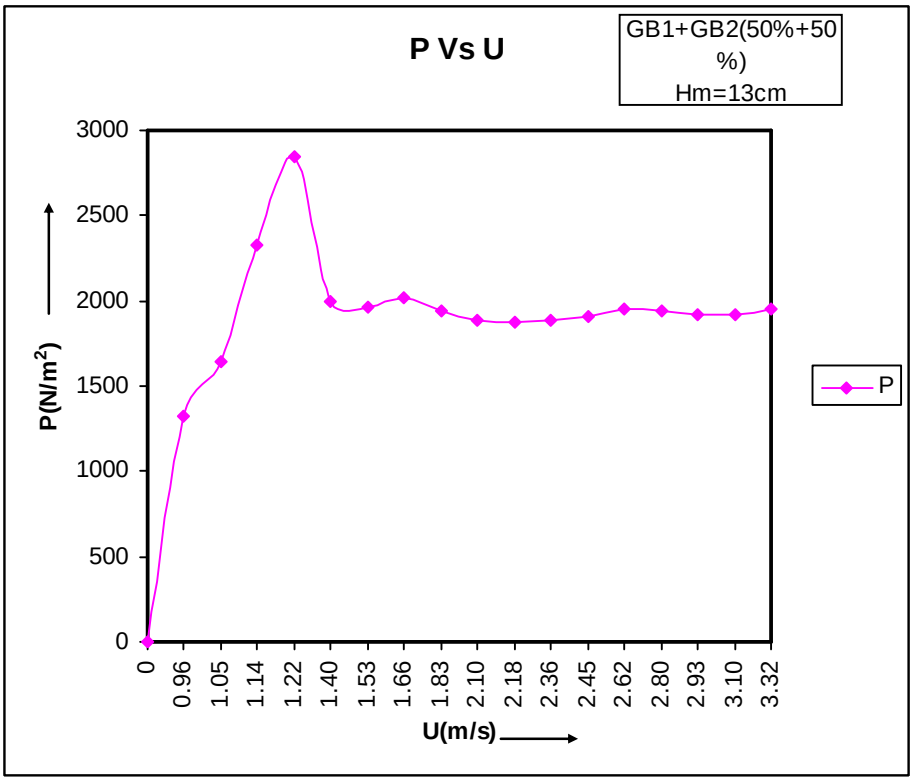

Fig. 6.3 ΔP Vs U plot for a mixture of glass beads of GB1(50%) and GB2 (50%)

Table 6.4:

Glass beads (Size: BSS -8+12 (25%) and BSS -12+14 (75%), Bed height=13cm)

$Q(m^3/hr)$	U(m/s)	P(cm)	$\Delta P(N/m^2)$
0	0	0	0
5	0.87	11.1	1733.82
6	1.05	15.1	2358.62
6.5	1.14	19.2	2999.04
7	1.22	14	2186.8
7.5	1.31	12.9	2014.98
8	1.40	12.8	1999.36
9.5	1.66	12.9	2014.98
10	1.75	12.9	2014.98
11	1.92	12.8	1999.36
12	2.10	12.8	1999.36
12.5	2.18	12.7	1983.74
14	2.45	12.8	1999.36
15	2.62	12.8	1999.36
16	2.80	12.8	1999.36

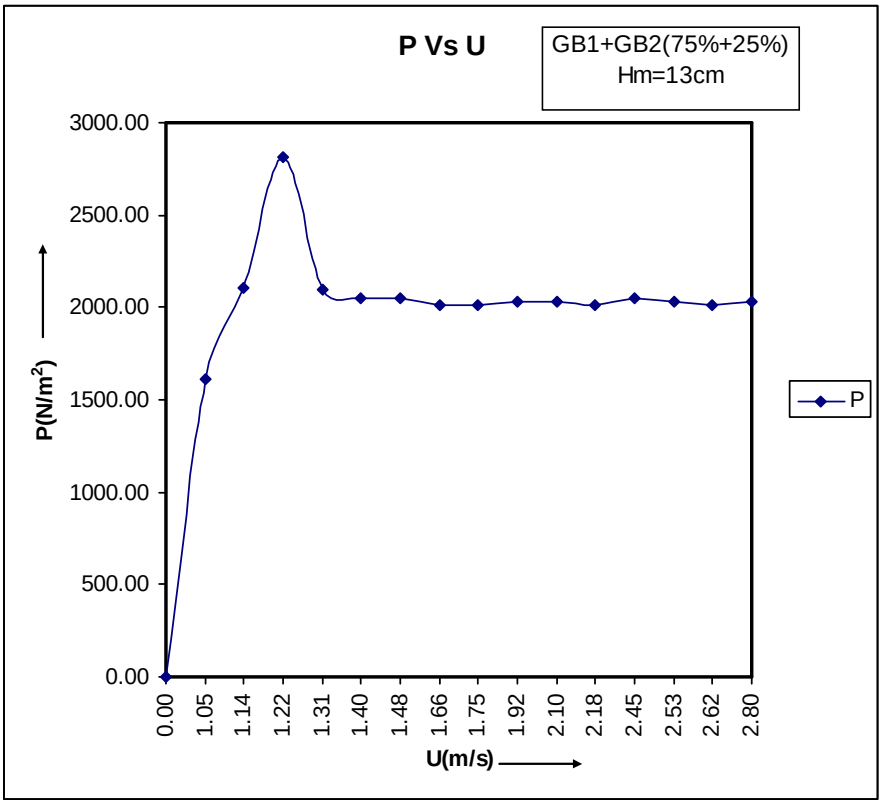

Fig. 6.4 ΔP Vs U plot for a mixture of glass beads of GB1 (25%) and GB2 (75%)

Table 6.5:

Glass beads (Size: BSS -8+12 (75%) and BSS -12+14 (25%), Bed height=13cm)

$Q(m^3/Hr)$	U(m/s)	P(cm)	$\Delta P(N/m^2)$
0	0.00	0	0.00
6	1.05	10.3	1608.86
6.5	1.14	13.5	2108.70
7	1.22	18	2811.60
7.5	1.31	13.4	2093.08
8	1.40	13.1	2046.22
8.5	1.48	13.1	2046.22
9.5	1.66	12.9	2014.98
10	1.75	12.9	2014.98
11	1.92	13	2030.60
12	2.10	13	2030.60
12.5	2.18	12.9	2014.98
14	2.45	13.1	2046.22
14.5	2.53	13	2030.60
15	2.62	12.9	2014.98
16	2.80	13	2030.60

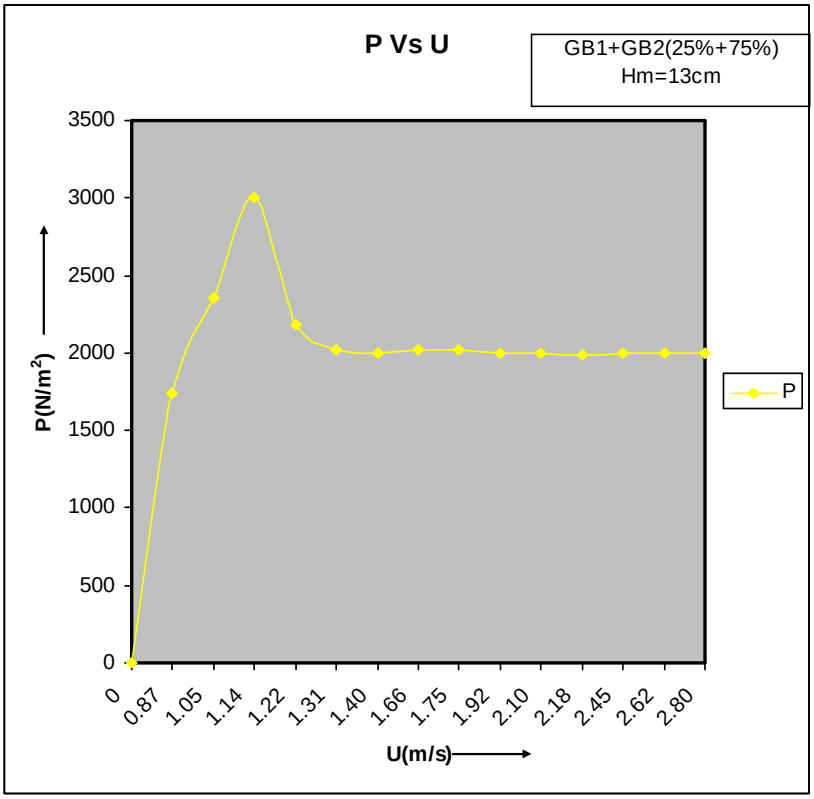

Fig. 6.5 ΔP Vs U plot for a mixture of glass beads of GB1(75%) and GB2 (25%)

Table 6.6:

Dolomite (Size: BSS -8+12, Bed height=13cm)

$Q(m^3/hr)$	P(cm)	$P(N/m^2)$	U(m/s)
0	0	0.00	0.00
5.25	6	937.20	0.92
10	9.3	1452.66	1.75
10.5	12	1874.40	1.83
13	18.5	2889.70	2.27
15.25	11.9	1858.78	2.66
16.5	11.5	1796.30	2.88
17	11.4	1780.68	2.97
17.75	10.7	1671.34	3.10
18.5	11.3	1765.06	3.23
19.25	11.3	1765.06	3.36
20	11.1	1733.82	3.49
22	11.3	1765.06	3.84

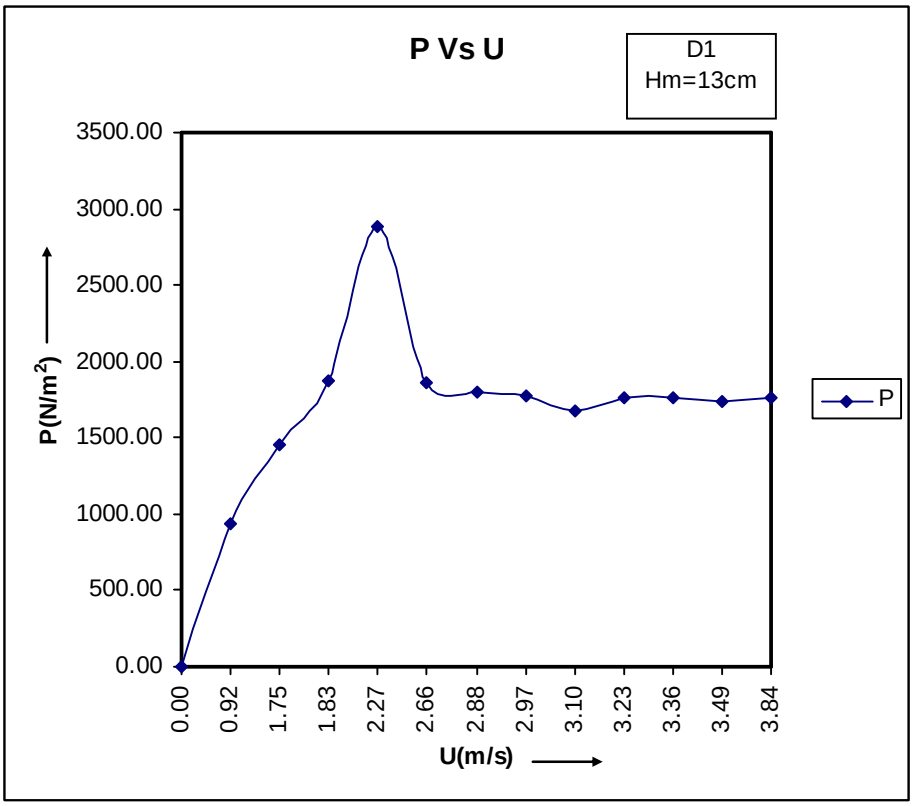

Fig. 6.6 ΔP Vs U plot for dolomite of -8+12 mesh size

6.2. MIXING –SEGRAGATION :

Table 6.7: Wt. % of dolomite

Dolomite (-12+14) (50%) and Dolomite (-16+18) (50%)

Static Bed Height = 13 cm

Height	D2 (wt. %)	D1(wt %)
4-6 cm	62.361	37.639
6-8 cm	60.909	39.091
8-10 cm	60.239	39.761
10-13 cm	53.384	46.616

Table 6.8: Wt. % of glass

Glass (-12+14) (50%) and Glass (-14+16) (50%)

Static Bed Height = 9 cm

Height	G3 (wt. %)	G4 (wt %)
0-3 cm	41.082	58.918
3-5 cm	44.277	55.723
5-7 cm	42.818	57.182
7-9 cm	25.042	74.958

Table 6.8: Wt. % of glass

Glass (-12+14) (50%) and Glass (-14+16) (50%)

Static Bed Height = 12.8 cm

Height	G3 (wt. %)	G4 (wt %)
4-6 cm	46.355	53.645
6-8 cm	36.498	63.502
8-10 cm	37.783	62.217
10-12.8 cm	42.549	57.451

6.3. CFD RESULTS:

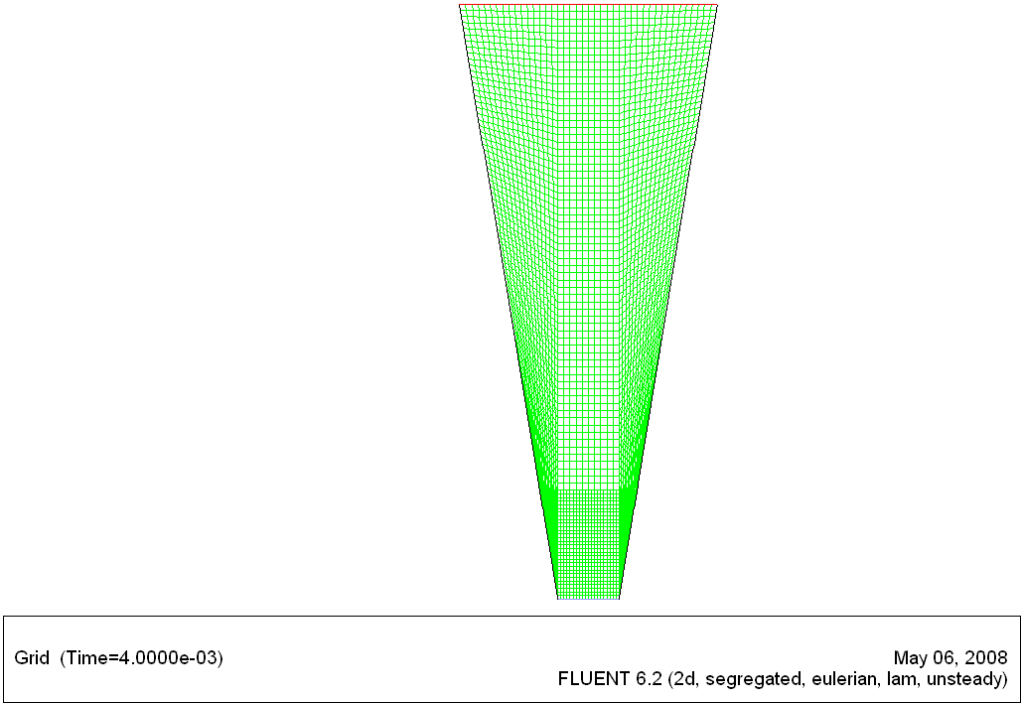

Fig. 6.7 Grid generated using GAMBIT 2.0.30

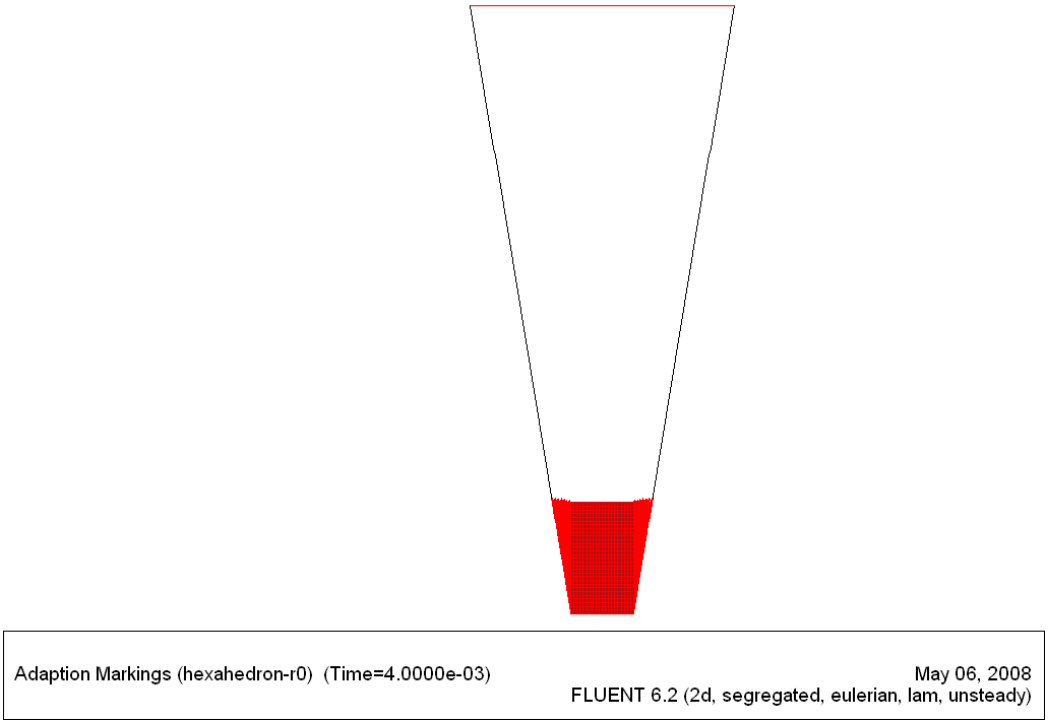

Fig. 6.8 The adaption region

Contours of Volume fraction Glass:

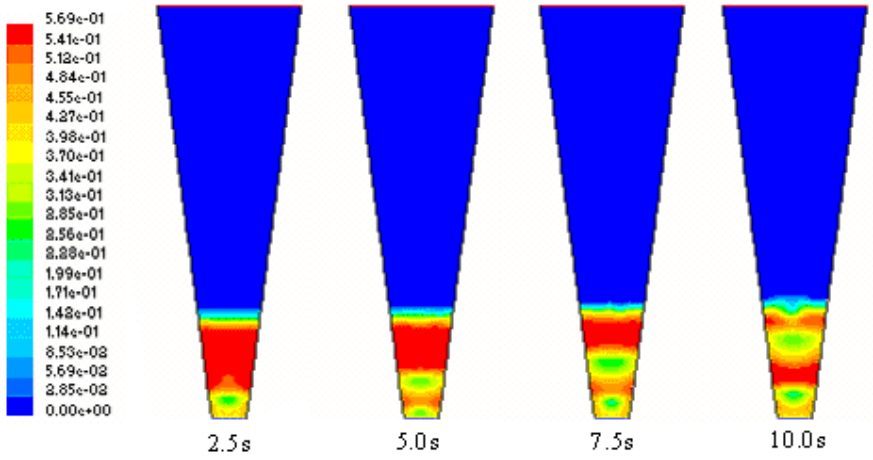

Fig. 6.9 Simulated solids volume fraction profile of 2D bed at minimum fluidization condition (U=Umf i.e.2.41m/s,particle=glass bead)

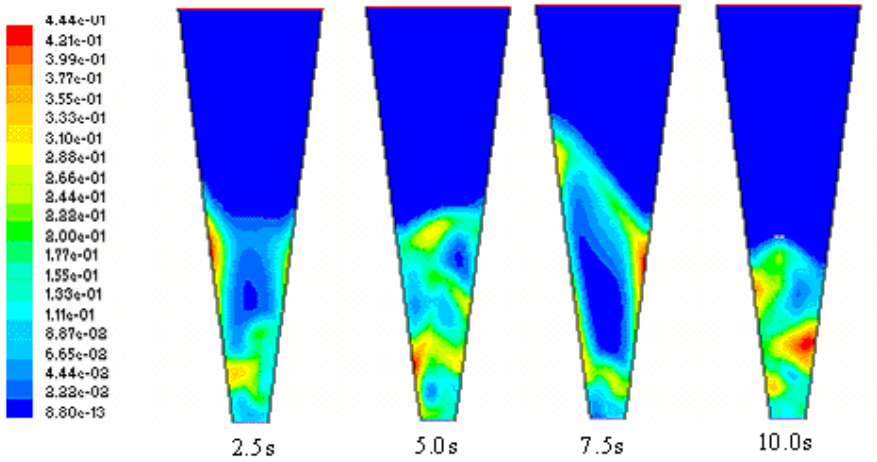

Fig. 6.10 Simulated solids volume fraction profile of 2D bed at fully fluidization condition (U=9.63m/s, i.e. ：4 Umf, particle=glass bead)

Contours of Volume fraction Dolomite:

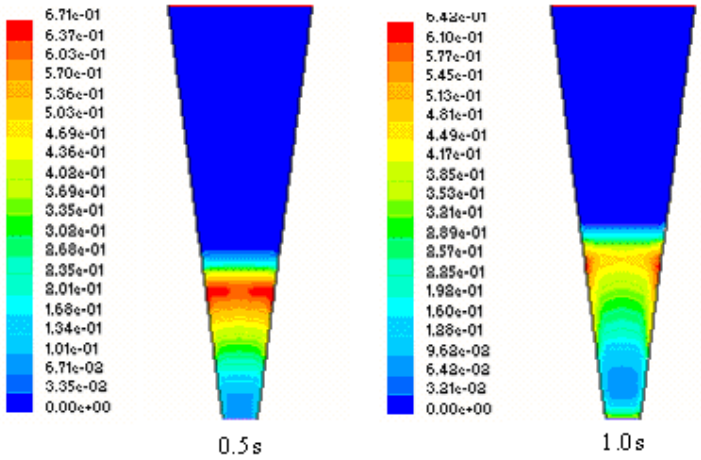

Fig. 6.11 Simulated solids volume fraction profile of 2D bed at minimum fluidization condition (U=Umf i.e.2.01m/s, particle=dolomite)

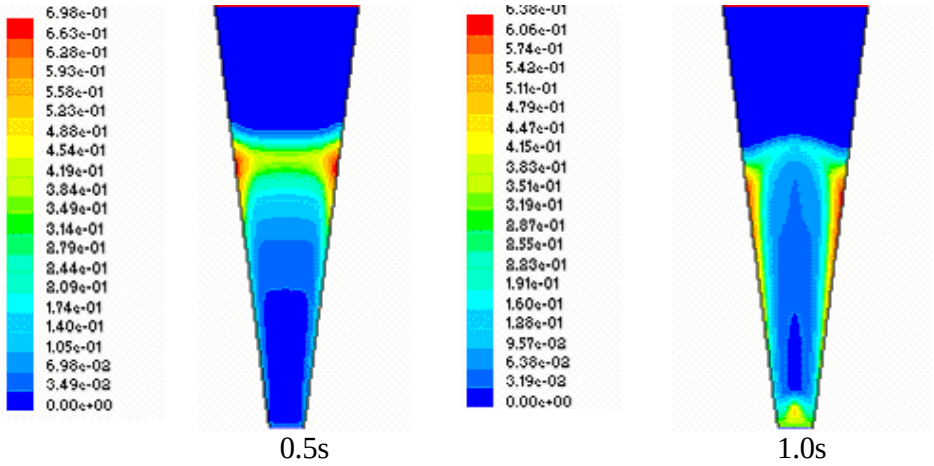

Fig. 6.12 Simulated solids volume fraction profile of 2D bed at fully fluidization condition (U= 4.01m/s, i.e. : 2Umf, particle=dolomite)

6.4. DISCUSSION :

- The hydrodynamic behavior of fluidization in tapered beds is best described by the plot of pressure drop across the bed versus superficial velocity of the fluid at the entrance.
- In the plots shown, from point A to point B, the pressure drop increases with the increase of superficial gas velocity. The transition from fixed bed to partially fluidized bed occurs at point B. From point B, the pressure drop decreases with the increase of superficial gas velocity and from point C, it remains constant.
- The velocity at point B is called critical fluidization velocity. At this point the pressure drop was maximum.
- Figures show the contours of solid and gas volume fraction along the length of the column. The diagrams obtained are useful in determining the material distribution in the column and also the pressure drop variation.
- For velocities of liquids below fluidization velocity, the solids didn't move much and it is a good result obtained.
- For minimum fluidization velocity, the diagram showed bed lifting after some time steps.
- Fluent has the ability to predict the results by simulating the given problem into software. Conducting the experiments involves a lot of cost. The results obtained were matching with the experimental one and hence Fluent is able to save the material and equipment cost; at the same time it gives us the flexibility to change the equipment dimensions and material properties. So a pilot scale experiment can be converted into an industrial one with the support from Fluent.

CHAPTER 7

CONCLUSIONS

7.1.**CONCLUSIONS :**

From the experimental results obtained, it can be inferred that pressure drop across the bed increases with increase in stagnant bed height. The critical fluidization velocity for the mixture decreases with increase in the weight fraction of flotsam in the mixture and a small increase in the maximum pressure drop was also observed with increase in the weight fraction of flotsam particles in the mixture.

A computational fluid dynamics model has been presented where the kinetic theory of granular flow forms the basis for the turbulence modeling of the solid phases. A multiphse Eulerian model integrating the kinetic theory for solid particles using Fluent software was capable of predicting the gas–solid flow behavior of a tapered fluidized bed. Comparison of the model predictions, using the Gidaspow drag functions, and experimental measurements on the time-average bed pressure drop and qualitative gas–solid flow pattern indicated reasonable agreement for most operating conditions. Good agreement of solid volume fraction profile was obtained between the experimental results and simulation results for glass bead (regular) particle but some differences were obtained for dolomite particles (irregular). However the current results are for two-dimensional only, and can therefore only serve to get a qualitative insight into the physical underlying of the fluidization behavior in tapered bed. For a true, quantitative comparison with experiments, clearly, full 3D simulations with different drag model (for irregular particles) are required.

7.2. FUTURE WORK:

Further work can be carried out for a mixture of particles of different densities as Flotsam and jetsam particles density is an important parameter. Quantitative comparison of the simulations with the experimental results can be done to further validate the utility of the technique.

NOTATIONS :

C_D	drag coefficient, dimemsionless
d_i	particle diameter, m
e_{ss}	restitution coefficient, dimensionless
g	acceleration due to gravity, m/s^2
$g_{0,ss}$	radial distribution coefficient, dimensionless
GB1	glass bead of size -8+12 (BSS)
GB2	glass bead of size -12+14 (BSS)
H	expanded bed height, m
Hs	static bed height, m
$\bar{\bar{I}}$	stress tensor, dimensionless
I_{2D}	second invariant of the deviatoric stress tensor, dimensionless
$k_{\Theta s}$	diffusion coefficient for granular energy, kg/s m
K_{gs}	gas/solid momentum exchange coefficient, dimensionless
K_a	coefficient, dimensionless
K_c	coefficient, dimensionless
P	pressure, Pa
Re	Reynolds number, dimensionless
$S_{s,a}$	solid phase source term for annulus, $kg/m^2\ s^2$
$S_{s,c}$	solid phase source term for core and hump, $kg/m^2\ s^2$
t	time, s
U	superficial gas velocity, m/s
v_i	velocity, m/s

v_s'	particle velocity fluctuation, m/s
z	height coordinate measured from distributor, m
ε_i	voidage, dimensionless
Θ_i	granular temperature,m^2/s^2
λ_i	bulk viscosity, kg/m.s
μ_i	shear viscosity kg/m.s
ρ_i	density kg/m^3
$\overline{\overline{\tau}}_i$	stress tensor, Pa
τ_p	particle relaxation time, s
$\gamma_{\Theta s}$	collision dissipation of energy, kg/s^3 m
ϕ_{gs}	transfer rate of kinetic energy , kg/s^3 m

Subscript

fb	fully fluidized
g	gas
i	general index
mf	minimum fluidization
max	maximum
o	fixed bed condition
s	solids
T	stress tensor

REFERENCES:

1. Agarwal, S.K.; and Roy, G K; Packed Bed Pressure Drop and Incipient Fluidization Condition in a Conical Bed of Spherical Particles – A Mathematical Model. Indian Chemical Engineer, vol 30, no 3, 1998, p 3.
2. Babu, S. P., Leipsiger, S., Lee, B. S., Weil, S. A. (1973), 'Solids mixing in batch operated tapered bed and non- tapered gas fluidized beds'. *Fluidized Bed Fundam. Appl*. AIChE Symp.Ser.69, 49-57.
3. Biswal K.C., Sahu, S., Roy, G. K. (1982), 'Prediction of fluctuation ratio for gas solid fluidization of regular particles in conical vessels', *The Chemical Engineering Journal*, 23,p 97-100.
4. Biswal, K.C.; Bhowmik, T.; Roy, G.K.; Prediction of pressure drop for a conical fixed bed of spherical particles in gas–solid systems, Chem. Eng. J. 29 (1984) 47–50.
5. Biswal.K.C, Samal, B. B., Roy G. K. (1984), 'Dynamics of gas-solid fluidization of regular particles in conical vessels', *The Journal the IE (India)*, Vol. 65, CH-1, 15 - 17.
6. Biswal, K.C. ; Bhowmik, T.; Roy, G.K.; Prediction of minimum fluidization velocity for gas–solid fluidization of regular particles in conical vessels, Chem. Eng. J. 30 (1985) 57–62.
7. Biswal K.C. and Roy G. K. (1985), 'Prediction of fluctuation ratio for gas-solid fluidizations of irregular particles in conical vessels'. *The Journal of the IE (India)*, Vol. 65, CH-2, 57-62.
8. Chiba,S., Nienow, A.W.,T.Chiba, Powder Technology,26,(1980),1~10
9. Cooper, S. and Coronella, C. J.; 'CFD simulations of particle mixing in a binary fluidized bed', Powder Technology, vol. 151, Issues 1-3, 2005, p 27-36.

10. Depypere, F.; Pieters, J.G.; Dewettinck, K.; Expanded bed height determination in a tapered fluidized bed reactor, Journal of Food Engineering 67 (2005) 353 – 359.
11. Enwald, H.; Almstedt, A.E.; "Fluid dynamics of a pressurized fluidized bed: comparison between numerical solutions from two-fluid models and experimental results", Chemical Engineering Science 54,329-342, (1999).
12. Fluent Inc.,"Fluent 6.1 UDF Manual"(2003a)
13. Fluent Inc.,"Fluent 6.1 user guide"(2003b)
14. Gibilaro,L.G. and Rowe ,P.N.: A model for a segregating gas fluidized bed; Chemical Engineering science,29,(1974) 1403
15. Gidaspow, D., Multiphase Flow and Fluidization. Academic Press, San Diego. 1994.
16. Gorshtein, A.E.; Mukhlenov, I.P.; Hydraulic resistance of a fluidized bed in a cyclone without a grate. II. Critical gas rate corresponding to the beginning of a jet formation, Zh. Prikl. Khim. (Leningrad) 37 (1964) 1887–1893.
17. Hoomans, B.P.B., Kuipers, J.A.M., Van Swaaij, W.P.M., 2000. Granular dynamics simulation of segregation phenomena in bubbling gas-fluidized beds. Powder Technology 109, 41–48.
18. Jing, S.; Hu, Q.; Wang, J.; Jin, Y.; Fluidization of coarse particles in gas–solid conical beds, Chem. Eng. Process. 39 (2000) 379–387.
19. Kim, H.G.; Lee, I.O.; Chung, U.C.; Kim, Y.H.; "Fluidization characteristics of iron ore fines of wide size distribution in a cold tapered gas-solid fluidized bed", ISIJ International,40, 16-22,(2000).
20. Koloini T. and Farkas E. J. (1973), 'Fixed bed pressure drops a liquid fluidization in tapered or conical vessels'. *Canadian Journal of Chemical Engineering*, 51, 499-502.
21. Kumar, A; Roy, G K; Institute of Engineers-India chemical engg division vol 84 (march 2004) 55-58.

22. Kunii, D.; and Levenspiel, O.; Fluidization Engineering, Wiley, New York, 1969
23. Lun, C.K.K.;Savage, S.B.; Jeffrey, D.J.; Chepurniy, N.; "Kinetic theories for granular flow: inelastic particles in couette flow and slightly inelastic particles in a general flow field", Journal of Fluid Mechanics,140,223-256,(1984).
24. Maruyama, T.; Sato, H.; Liquid fluidization in conical vessels, Chem. Eng.J. 46 (1991) 15–21.
25. Maruyama, T.; and Koyanagi, T.; Fluidization in Tapered Vessels, Chemical Engineering Journal, vol 52, 1993, p 121.
26. Maruyama, T ; and Koyanagi, T; Slugging Fluidized Beds in Tapered Vessels. Chemical Engineering Journal, vol 52, 1993, p 99.
27. Naimer, N.S.; Chiba, T.; and Nienow, A.W, Parameter estimation for a solids mixing /segregation model for gas fluidized beds; Chemicalengg. Communication, 62(1987),53.
28. Nienow, A.W., Chiba, T., 1981. Solid mixing and segregation in gas-fluidized Beds. The Institution of Chemical Engineers Symposium Series, vol. 65. Mixing of Particulate Solids, pp. S2/F/1-S2/F-19
29. Nishi, Y.; Kagaku kogaku Ronbunshu 5 (1979) 202–204.
30. Olazer, M; San Jose, M.J.; Aguayo, A.T.; Arandes, J.M.; Bilbao, J.; Pressure drop in conical spouted beds, The Chemical Engineering Journal 51 (1993) 53 – 60.
31. Peng, Y.; Fan, L.T.; Hydrodynamic characteristics of fluidization in liquid-solid tapered beds, Chemical Engineering Science, vol 52, no 14, 1997, p 2277 – 2290.
32. Renzo DiFelice, Piero U. Foscolo, Larry G. Gibilaro, Graham B. Wallis and Renzo Carta, 'Expansion Characteristics of Tapered Fluidized Beds', AIChE Journal, vol. 37, no. 11, 1991, p 1668-1672.

33. Schaafsma, S H; Marx, T.; and Hoffmann, A C; Investigation of the particle flow pattern and segregation in tapered fluidized bed granulators, Chemical Engineering Science, Vol 61, Issue 14, 2006, p 4467-4475.
34. Scott, C.D.; Hancher, C.W. ; Use of a tapered fluidized bed as a continuous bioreactor, Biotechnol. Bioeng. 18 (1976) 1393–1403.
35. Shan, J.; Guobin, C.; Fan, M.; Yu, B.; Jingfu, W.; Yong, J.; Fluidization of fine particles in conical beds, Powder Technology 118 (2001) 271 – 274.
36. Shi, Y.F.; Yu, Y.S.; Fan, L.T.; "Incipient fluidization condition for a tapered fluidized bed", Ind. Eng. Chem. Fundam., 23, 484 – 489, (1984).
37. Singh, R.K.; Suryanarayana, A.; Roy, G.K.; Prediction of minimum velocity and minimum bed pressure drop for gas–solid fluidization in conical conduits, Can. J. Chem. Eng. 70 (1992) 185–189.
38. Syamlal M.; O'Brien T.J.; "Computer simulation of bubbles in a fluidized bed", A.I.Ch.E. Symposium Series 85, 23-31,(1989).
39. Toyohara and Kawamura. Fluidization of Tapered Bed of a Binary Particle Mixture. International Chemical Engineering, vol 32, no.1, 1992, p 164.
40. Wu, S.Y and Baeyens, J.; Segregation by size difference in gas fluidized beds; Powder Technology, 98(1998)139

APENDIX 1:

Boundary conditions used for the simulation of tapered fluidized bed

Description	Type	Comments
Inlet	Velocity-inlet	Uniform distribution for gas phase
		No particles enter for solid phase
Outlet	Pressure-outlet	Atmospheric
Wall	Stationary wall	No slip for gas phase
		Zero shear stress for solid phase

APENDIX 2:

Parameters used for CFD simulation of tapered bed

Description	Value	Comment
Inlet gas velocity,Ui(m/s)	0 : 9.63	Uniform distribution
Gas density(kg/m^3)	1.17	Air
Gas viscosity(kg/m.s)	1.83×10^{-5}	Air
Particle density(kg/m^3)	2600, 2800	Glass bead, Dolomite
Particle diameter(mm)	2.61,1.54	Uniform distribution
Initial solids packing	0.554,0.74	Fixed value
Packing limit	0.57,0.76	Fixed value
Solid viscosity	Gidaspow	
Solid bulk viscosity	Lun et al.	
Bottom diameter of the bed	0.042	Fixed value
Top diameter of the bed	0.174	Fixed value
Total height of the column	0.504	Fixed value
Static bed height	0.115	Fixed value
Solver	Double precision, segregated, unsteady, 1^{st} order implicit;	
Model	2D,Eulerian, 2 phases	
Viscous Model	Laminar	
Phase Interaction	Fluid –solid exchange coefficient :Gidaspow model	
Restitution coefficient	0.9	
Time steps (s)	0.001 : 0.0002	Fixed value
Convergence criterion	0.001	Default in FLUENT